FIRST-PRINCIPLES INVESTIGATION THE PHASE SEPARATION IN $Ca_{1-x}Mg_xO$ ALLOYS

R. Miloua, F. Miloua, Z. Kebbab, N. Benramdane

Laboratoire d'Elaboration et de Caractérisation des Matériaux,
Faculté des Sciences de l'Ingénieur, BP 89, Université Djillali LIABES
Sidi-Bel-Abbès, Algeria.
Tel: 00 213 50 71 61 56; E-mail: mr_lecm@yahoo.fr

Using the full-potential linearized augmented plane wave (FP-LAPW) method in combination with the local density approximation to the exchange-correlation potential, we investigated the ground-state properties and the stability of $Ca_{1-x}Mg_xO$ mixed oxides. It is found that the structural parameters, i.e. lattice constants and bulk moduli deviate slightly from the linear function of the composition *x*. We determined the equation of state of the alloys and showed an increasing compressibility function of composition. We expressed the formation energy as an energetic balance between pure structural constraints and quantum chemical effects. Thus, a phase separation over the whole range of concentration is expected. The origin of the miscibility gap has a chemical nature. Also, we performed a thermodynamic study of the stability of the alloys.

Keywords: development and study of material properties to form catalytic layers in fuel cells, new structural materials for renewable energy structures

F. Miloua

Organization(s): Scientist researcher at Laboratoire d'Elaboration et de Caractérisation des Matériaux.
Education: D.E.A in electronics at Université des Sciences et Techniques of Lille, France (1986). Doctorate in Physics and materials science at Claude Bernard University- Lyon I, France (1992).
Main range of scientific interests: Materials science, surfaces and interfaces.
Some publications (number of publications: 11)**:** F. Miloua et al. Structural and electrical characterzation of Ag-InP(100) interfaces stabilized by antimony // Materials Chemistry and Physics 1993. 33. P. 85.; M. Bouslama, B. Khelifa, F. Miloua et al. Interaction of phosphorus with Indium // Appl. Surf. Sciences. 1992.; F. Miloua et al. Structural and electrical characterizations of Ag-InP(100) interfaces stabilized by antimony // 3ème Rencontre de Physique: ''Sciences des Surfaces des Matériaux''. Oran. 1991.

Introduction

The alkaline earth oxides CaO and MgO, as well as their mixtures have been in focus both theoretically and experimentally. Because of their interesting physical and chemical properties, they found a wide range of applications ranging from catalysis to microelectronics. They have been used as catalysts for the steam gasification of naphthalene [1], in oxidative coupling reaction of methane [2] and for soot combustion [3]. Recently, $Ca_{1-x}Mg_xO$ solid solutions have been demonstrated as an alternative dielectrics to SiO_2 due to favourable properties such as high dielectric constant, wide bandgap, and notable lattice compatibility with SiC [4]. CaMgO films grown by rf plasma-assisted molecular beam epitaxy and capped with Sc_2O_3 are promising candidates as surface passivation layers and gate dielectrics on GaN-based high electron mobility transistors (HEMTs) and metal-oxide semiconductor HEMTs (MOS-HEMTs) [5, 6].

Due to the large difference in ionic radius between Mg and Ca, solid-solution CaO-MgO is difficult to synthesize using bulk techniques, i.e. a severe immiscibility is observed [7]. However, the use of MBE as a film growth technique often allows for the formation of metastable phases. In fact, $Ca_{1-x}Mg_xO$ ternaries were grown as solid solution films covering the entire compositional range when grown at a remarkably low temperature of 300 °C [8]. Also, using pulsed laser deposition, Nishii et al. have grown metastable solid solution films on ZnO layers [9].

In the present paper we report on the structural and thermodynamic stability of $Ca_{1-x}Mg_xO$ alloys. We employed the Full-Potential Linearised Augmented Plane Wave (FP-LAPW) method [10] to study the ground-state properties and the formation energy of the alloys. The disordering effect on the formation energy is introduced using a cluster expansion approach. The predicted trends are explained on the basis of a structural-chemical energetic balance. Further, the thermodynamic phase diagram is established and the critical temperature is estimated.

The rest of the paper is organized as follows. In section 2, we briefly describe the calculation procedure. Results and discussions are presented in section 3 and the paper is concluded in section 4.

Method of calculation

Our calculations have been made using FP-LAPW approach within the framework of the Density Functional Theory (DFT) [11, 12] as implemented in WIEN2k [13] code. The exchange-correlation contribution to the total energy is described within the Local Density approximation (LDA) [14]. Kohn-Sham wave functions were expanded in terms of spherical harmonic functions inside the non-overlapping muffin-tin spheres surrounding the atomic sites (MT spheres) and in Fourier series in the interstitial regions. Inside the MT spheres of radius R_{MT}, the l-expansion of the wave function were carried out up to $l_{max} = 10$ while the charge density was Fourier expanded up to $G_{max} = 14$ (Ryd)$^{1/2}$. In order to achieve energy eigenvalues convergence, the wave functions in the interstitial region were expanded in plane waves with a cut-off parameter of $K_{max} = 8/R_{MT}$ for both binary and ternary compounds. R_{MT} values were assumed to be 2.0 a.u. for Mg, 2.2 a.u. for Ca and 1.6 a.u. for O atoms, respectively for all structures. A mesh of 30 special k-points for both binary and ternary compounds was taken in the irreducible wedge of the Brillouin zone. Both the MT radius and the number of k-points were varied to ensure total energy convergence. The core states that are completely confined inside the corresponding MT spheres were treated fully relativistic, while for the valance states we used the scalar relativistic approach that includes the mass velocity and Darwin s-shift, but omits spin-orbit coupling.

Results and discussions

Structural parameters

First, we calculated the structural properties of the binary compounds CaO and MgO in the rock-salt structure. Then, the ordered ternary alloys $Ca_{1-x}Mg_xO$ ($0 \le x \le 1$) were simulated at compositions $x = 0.25$, 0.5 and 0.75 by substituting cations. For each composition, we carried out a structural optimization by minimizing the total energy with respect to the cell volume and also the atomic positions. The calculated lattice constants and bulk moduli (see Table 1) were obtained by fitting the total energy versus unit cell volume to the Murnaghan's equation of state [15].

Table 1

Calculated lattice constants and bulk moduli, compared to experimental and other theoretical results

$Ca_{1-x}Mg_xO$	Lattice constants, a (Å)			Bulk moduli (GPa)		
x	This work	Exp	Other calc	This work	Exp	Other calc
0	4.71	4.81 [16]	4.72 [17]	127	110 [16]	128 [17]
0.25	4.61			135.84		
0.5	4.49			144.41		
0.75	4.35			157.12		
1	4.17	4.213 [18]	4.165 [17]	173.15	160 [18]	171 [17]

In Fig. 1 and Fig. 2 we depicted, respectively the lattice constants and the bulk moduli as a function of the composition x. From Fig. 1, one can see that the calculated lattice parameters deviate slightly from those obtained from the Vegard's law. The differences between themes are less than 5.5 %. The calculated lattice constants follow a decreasing quadratic function of composition x

$$a(x) = 4.70961 - 0.32582x - 0.21422x^2. \quad (1)$$

In Fig. 2, the composition dependence of the bulk moduli is compared with the results predicted by the linear concentration dependence (LCD). The bulk moduli exhibit a strong deviation from the LCD. Considering the general trend that LDA usually underestimates the lattice constant and overestimates the bulk modulus, our results are in good agreement with the experimental and other calculated values (see Table 1).

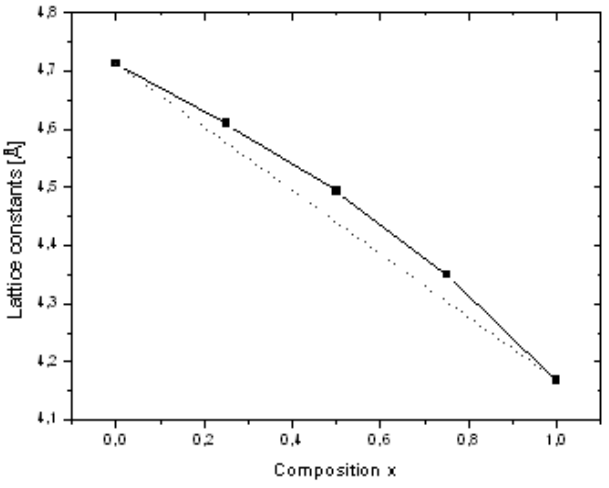

Fig. 1. *The calculated lattice constants (solid squares) and lattice constants of ideal mixing solid solutions (doted line) for the five ordered structures $Ca_{1-n}Mg_nO$ (n = 0, 1, 2, 3, 4)*

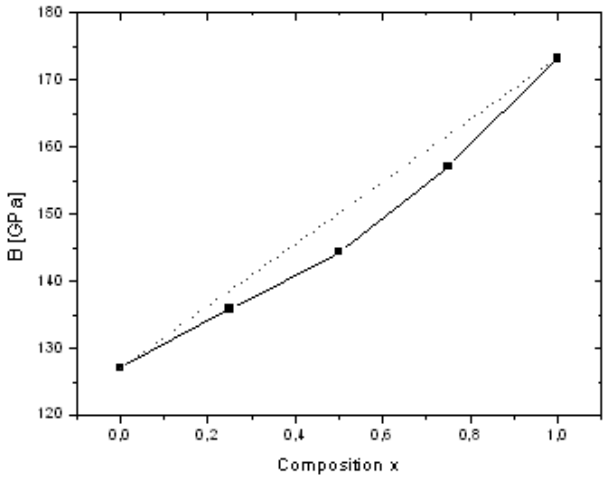

Fig. 2. *Calculated bulk moduli (solid squares) and those of ideal mixing (dotted line) as a function of composition*

Equation of state

The calculated equation of state for the $Ca_{1-x}Mg_xO$ alloys is plotted in Fig. 3. The relationship of the strain volume V/V_0 (where V is the unit cell volume under pressure, V_0 is the volume without pressure) under the same pressure P among the different compositions can be written as

$$(V/V_0)_{CaO} < (V/V_0)_{Ca_3MgO_4} < (V/V_0)_{CaMgO_2} < < (V/V_0)_{CaMg_3O_4} < (V/V_0)_{MgO}. \quad (2)$$

The relationship shows that CaO can be compressed more easily than MgO, this trend is observed in the bulk modulus ($B_{CaO} < B_{MgO}$). The compressibility decreases when the composition x increase.

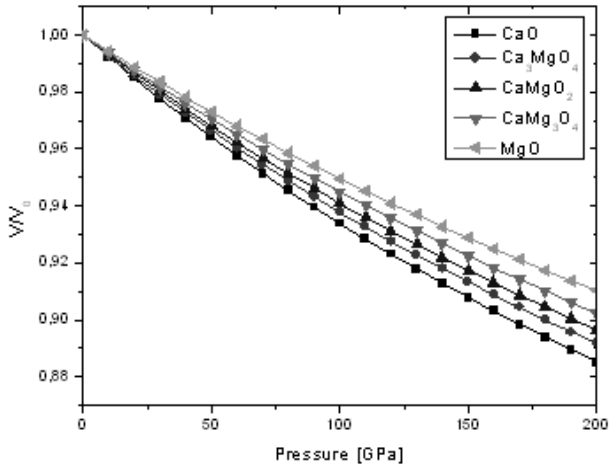

Fig. 3. *Equations of state of the $Ca_{1-x}Mg_xO$ alloys*

Phase separation of the CaMgO alloys

The ordered phases

In order to study the stability of CaMgO in the ordered form, we calculated the formation energies of the five (n = 0, 1, 2, 3, 4) structures using the following relation

$$E_{form}(n) = E_{Ca_{1-n}Mg_nO} - \frac{n}{4}E_{MgO} - \left(1 - \frac{n}{4}\right)E_{CaO}, \quad (3)$$

where $E_{Ca_{1-n}Mg_nO}$ is the total energy of the nth ordered alloy, E_{MgO} and E_{CaO} are total energies of MgO and CaO binaries, respectively. The results are viewed in Fig. 4 (solid squares) together with those for disordered alloys (solid line).

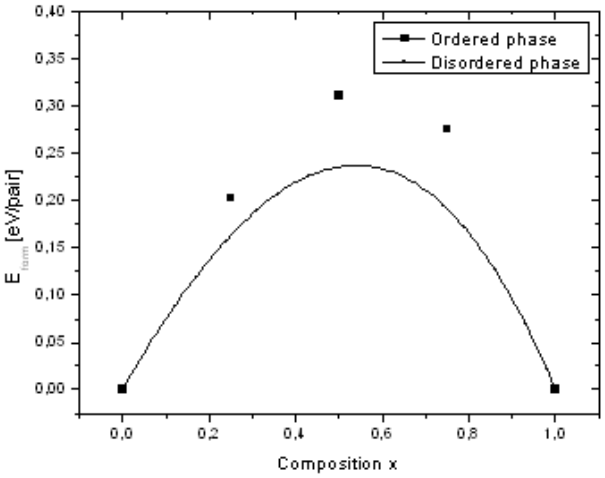

Fig. 4. *The calculated formation energies for ordered structures and disordered alloys*

The formation energy can give a measure of the stability of a material. We notice that it is positive for the whole range of composition, this indicates that it is energetically unfavourable for CaO and MgO to mix and form alloys. In order to clarify the physical origin of this behaviour, we decompose E_{form} into three physically recognizable contributions [19-21] as follows:

$$E_{form} = E_{VD} + E_{CE} + E_{SR}, \quad (4)$$

where E_{VD} is the hydrostatic "volume deformation" contribution due to the dilatation of MgO and compression of CaO from their equilibrium lattice constants (4.17 Å and 4.71 Å, respectively) to the common (Vegard-like) lattice constant of the alloy;

E_{CE} is the "charge exchange" energy that releases when MgO and CaO, taken at common lattice constant, combine to give $Ca_{1-x}Mg_xO$ ordered alloy. The internal relaxation effects are not included in this energy.

E_{SR} is the "structural relaxation" term due to the full relaxation of cell-internal degrees of freedom.

Fig. 5 shows the splitting of the formation energies of the ternary alloys into the three physical contributions; we can deduce the following important remarks:

– The large lattice mismatch (≈ 12%) between the binary constituents leads to a large and positive E_{VD} that tends to decrease the stability of CaMgO alloys over the whole range of composition.

– In contrast to E_{VD}, internal relaxation tends to increase the stability of the alloys by taking a negative E_{SR} value. However, E_{SR} is very small, compared to E_{VD} and the sum $E_{VD} + E_{SR}$ remains positive.

– The E_{CE} contribution remains positive and is higher than $E_{VD} + E_{SR}$, so can say that the phase separation has a chemical nature.

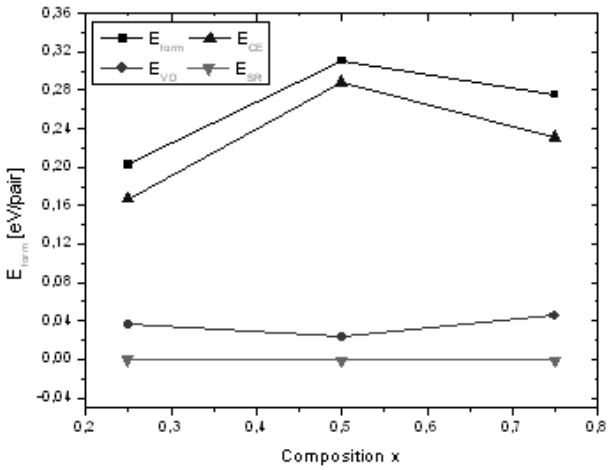

Fig. 5. *Energy contributions to the formation energies of ordered alloys*

The disordered phase

In this section, the energetic properties of the disordered alloys are calculated using a cluster expansion method. Following the idea of Connolly and Williams [22], the energy of formation of the disordered solid solutions can be written as

$$E_{form}^{dis}(x) = \sum_{n=0}^{4} P_n(x) E_{form}^{n}(x) \qquad (5)$$

$$P_n(x) = \binom{4}{n} x^n (1-x)^{4-n} \qquad (6)$$

where $E_{form}^{n}(x)$ is the energy of formation of each of the five ordered structures. $P_n(x)$ is a statistical weight representing the probability that the nth short-range ordered structure occurs in the alloy. In Fig. 4 (solid line), the formation energy of the disordered alloys is depicted. It is lower than that of the ordered structures.

Thermodynamic properties

The thermodynamic properties of $Ca_{1-x}Mg_xO$ are calculated by estimating the solubility limit. Following the approach of Neugebauer and Van de Walle [23], we use the calculated formation energy to construct a lower limit $\Delta H^{\min}(x)$ for each composition

$$\Delta H^{\min}(x) = 4x(1-x)\Delta H^0, \qquad (7)$$

where $\Delta H^0 = 0.1351863$ eV ($\Delta H^{\min}(x) = 0.1013897$ eV with $x = 0.25$). Then, the miscibility gap is analytically estimated and its behaviour as a function of temperature is given by the binodal line, as shown in Fig. 6 (solid line) [24, 25]

$$k_B T / \Delta H^0 = (8x-4)/[\ln x - \ln(1-x)]. \qquad (8)$$

The region below the spinodal line is unstable (as indicated by doted line)

$$k_B T / \Delta H^0 = 8x(1-x). \qquad (9)$$

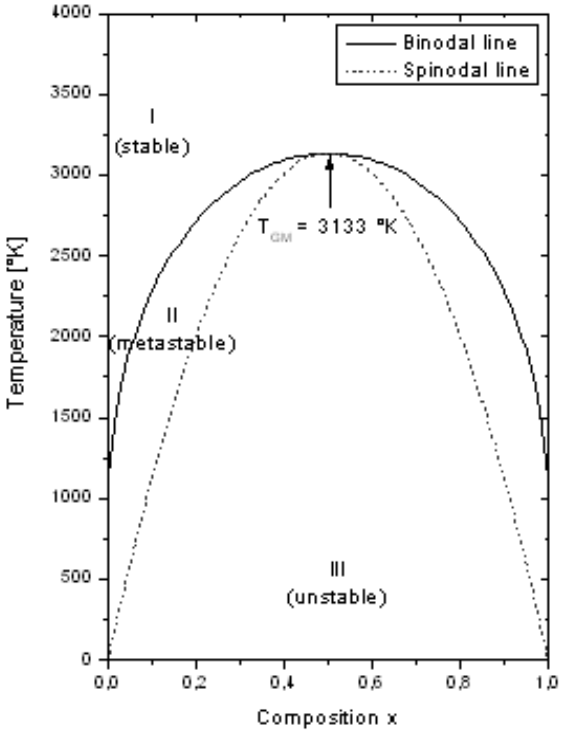

Fig. 6. *T-x phase diagram of $Ca_{1-x}Mg_xO$ alloys, solid line: binodal curve, doted line: spinodal curve*

The critical temperature of the miscibility gap is thus $T_{GM} = 2\Delta H^0/k_B = 3133$ K.

The spinodal curve in the phase diagram marks the equilibrium solubility limit, i.e., the miscibility gap. For temperatures and compositions above this curve a homogeneous alloy is predicted. The wide range between spinodal and binodal curves indicates that the alloy may exist as metastable phase.

Conclusion

In summary, we performed accurate FP-LAPW calculations to investigate the structure and the stability of $Ca_{1-x}Mg_xO$ solid solutions in the ordered and disordered forms. It is shown that the lattice constants and bulk moduli exhibit a strong deviation from the linear law. The compressibility of the alloys decreases when the composition x increase. The calculated formation energies for both ordered and disordered phases are positive and yield to a miscibility gap. Then, the origin of phase separation was determined to be of a chemical nature. Further, the thermodynamic phase diagram is calculated and a critical temperature of T_{GM} = = 3133 K is found.

References

1. Alarcón N., García X., Centeno M. et al. Catalytic cooperation at the interface of physical mixtures of CaO and MgO catalysts during steam gasification of naphthalene // Surface and Interface Analysis. 2001. 31. P. 1031.
2. Omata K., Aoki A., Fujimoto K. Oxidative coupling of methane over CaO-MgO mixed oxide // Catalysis Letters. 1990. 4. P. 241.
3. Jiménez R., García X., Gordon A. CaO-MgO catalysts for soot combustion: KNO_3 as source for doping with potassium // J. Chil. Chem. Soc. 2005. 50. P. 651.
4. Stodilka D.O., Gerger A.P., Hlad M. et al. Alternative magnesium calcium oxide gate dielectric for silicon carbide MOS application // Mater. Res. Soc. Symp. Proc. 2006. 911. P. 3.
5. Gila B.P., Thaler G.T., Onstine A.H. et al. Novel dielectrics for gate oxides and surface passivation on GaN // Solid-State Electronics. 2006. 50. P. 1016.
6. Hlad M., Voss L., Gila B.P. et al. Dry etching of MgCaO gate dielectric and passivation layers on GaN // Applied Surface Science. 2006. 252. P. 8010.
7. Doman R.C., Barr J.B., McNally R.N. et al. Phase equilibria in the system CaO-MgO // J. Am. Ceram. Soc. 1963. 46. P. 314.
8. Hellman E.S., Hartford E.H. Epitaxial solid-solution films of immiscible MgO and CaO // Appl. Phys. Lett. 1994. 64. P. 1341.
9. Nishii J., Ohtomo A., Ikeda M. et al. High-throughput synthesis and characterization of $Mg_{1-x}Ca_xO$ films as a lattice and valence-matched gate dielectric for ZnO based field effect transistors // Applied Surface Science. 2006. 252. P. 2507.
10. Andersen O.K. Linear methods in band theory // Phys. Rev. B 1975. 42. P. 3060.
11. Hohenberg P., Kohn W. Inhomogeneous Electron Gas // Phys. Rev. 1964. 136. P. B864.
12. Kohn W., Sham L.S. One-particle properties of an inhomogeneous interacting electron gas // Phys. Rev. 1965. 140. P. A1133.
13. Blaha P., Schwarz K., Madsen G.K.H. Electronic structure calculations of solids using the WIEN2k package for material sciences // Comput. Phys. Commun. 2002. 147. P. 71.
14. Ceperley D.M., Alder B.J. Ground state of the electron gas by a stochastic method // Phys. Rev. Lett. 1980. 45. P. 566.
15. Murnaghan F.D. The compressibility of media under extreme pressures // Proc. Natl. Acad. Sci. USA. 1944. 30. P. 244.
16. Richet P., Mao H.K., Bell P.M. Static compression and equation of state of CaO to 1.35 Mbar // J. Geophys. Res. 1988. 93. P. 15279.
17. Baltache H., Khenata R., Sahnoun M. et al. Full potential calculation of structural, electronic and elastic properties of alkaline earth oxides MgO, CaO and SrO // Physica B. 2004. 344. P. 334.
18. Fei Y. Effects of temperature and composition on the bulk modulus of (Mg,Fe)O // Am. Mineral. 1999. 84. P. 272.
19. Wei S.H., Ferreira L.G., Zunger A. First-principles calculation of temperature-composition phase diagrams of semiconductor alloys // Phys. Rev. B 1990. 41. P. 8240.
20. Satani M., Hart G.L.W., Zunger A. Ordering tendencies in octahedral MgO-ZnO alloys // Phys. Rev. B 2003. 68. P. 155210.
21. Bernard J.E., Zunger A. Electronic structure of ZnS, ZnSe, ZnTe, and their pseudobinary alloys // Phys. Rev. B 1987. 36. P. 3199.
22. Zunger A., Wei S.-H., Ferreira L.G. et al. Special quasirandom structures // Phys. Rev. Lett. 1990. 65. P. 353.
23. Connolly J.W.D., Williams A.R. Density-functional theory applied to phase transformations in transition-metal alloys // Phys. Rev. B 1983. 27. P. 5169.
24. Lambrecht W.R.L., Segall B. Electronic structure of (diamond C)/(sphalerite BN) (110) interfaces and superlattices // Phys. Rev. B 1989. 40. P. 9909.
25. Lambrecht W.R.L., Segall B. Anomalous band-gap behaviour and phase stability of c-BN–diamond alloys // Phys. Rev. B 1993. 47. P. 9289.